An observer-based fault-tolerant controller for flexible buildings-based on linear matrix inequality approach

Chaojun Chen[1], Zuohua Li[1], Jun Teng[1,*] and Ying Wang[2]

[1]School of Civil and Environment Engineering, Shenzhen Graduate School, Harbin Institute of Technology, Shenzhen 518055, China
[2]Department of Civil and Environmental Engineering, University of Surrey, Guildford, GU2 7XH, UK

Since failures in sensors degrade the performance of active mass damper (AMD) control systems, a dynamic filter design method, a state observer design method and a robust control strategy are developed and presented in this paper to overcome this deficiency. The filter design method is transformed into a H_2/H_∞ control problem that is solved by linear matrix inequality approach. Thus, it is used to perform fault detection and isolation (FDI) for the control systems. The state observer design method uses the acceleration responses as the feedback signal. The detected and isolated fault signals in accelerometers are used to estimate the whole states, that are used to calculate the control force though a robust control strategy based on regional pole-assignment algorithm. Then, the active fault-tolerant control (FTC) is accomplished. To verify its effectiveness, the proposed methodology is applied to a numerical example of a ten-storey frame and an experiment of a single span four-storey steel frame. Both numerical and experimental results demonstrate that the performances of FTC controller and the control system are improved by the designed dynamic FDI filter to effectively detect and isolate fault signal.

Keywords: AMD control system, fault-tolerant control, flexible buildings, fault detection and isolation, state observer.

ACTIVE mass damper (AMD) is used to control the dynamic response of highly flexible buildings horizontally[1–5]. Recently, several studies focused on robust controller design for nonlinear dynamical systems and mainly include fault-tolerant control (FTC) technology[6–9]. The design methods of the FTC system include analytical redundancy method, hardware redundancy method, etc. The hardware redundancy method aims to provide backup hardware for components that are prone to failure and to improve the fault-tolerant performance of the system. However, this method increases hardware costs and the weight of the system, and is restricted by space. Therefore, the analytical redundancy method, which improves the redundancy of the system through the design of the controller, is more appropriate for flexible buildings. The FTC system using analytical redundancy method is divided into passive and active fault-tolerant systems. The passive fault-tolerant system, which cannot accomplish on-line fault identification, is regarded as traditional robust control. In comparison, the active FTC system in engineering practices needs to utilize the dynamic fault detection and isolation (FDI) technology to contain fault signals. Currently, several innovative FDI technologies have been developed[10] and widely used in the field of control[11–14]. Generally, the AMD system of a high-rise building includes sensors, actuators and controller. In practice, structural vibration response measured by several types of sensors is sent to the controller as the feedback signal, which is usually a state vector composition of displacement and velocity in the horizontal direction[15,16]. Instead, using a state observer can overcome the deficiency when the whole states are too hard to be measured directly in a high-rise building. Since acceleration is easier to measure than displacement and velocity, it is used to construct the state observer that is more robust[17]. Based on the state observer and a suitable control strategy, the control system restrains the structural response in a timely manner[18,19]. Noticeably, due to adverse circumstances such as mechanical damage, environmental damage and lack of maintenance, the attached accelerometers may sometimes malfunction or even fail. An observer-based system is considered to introduce a fault signal that seriously reduces the control performance. Therefore, the reliability and robustness of this system should be studied. FDI technologies are often used to estimate the state of the control system through an observer. For example, Kalman filter was used to estimate the state of an aircraft model and also introduced for fault detection and isolation[20]. An observer-based FDI technology was designed to estimate the state of linear structural systems, so as to detect faults and disturbances of the systems[21]. In other studies[22], an observer with unknown input was applied to the system with random noise, which realized the fault detection and identification. However, a state observer design method based on the acceleration signals with a corresponding protective

*For correspondence. (e-mail: tengj@hit.edu.cn)

measure (a FDI filter), which is an effective measure for flexible buildings to resist strong dynamic loads, needs further theoretical and applied studies.

In this paper, the derivation of the state-space equation of flexible buildings with an AMD control system that considers fault signal in sensors is first described. The design problem of the dynamic FDI filter is then expressed as a group of nonlinear matrix inequalities that are transformed into a group of linear matrix inequalities (LMI)[23] through variable substitution method[24]. Through the FDI filter, the detected and isolated signal is regarded as the input of the designed state observer to estimate the whole states of the system, which are used to calculate the control force based on regional pole-assignment algorithm[25]. Finally, a numerical example of ten-storey frame and an experiment of a single span four-storey steel frame is presented to verify the effectiveness of the proposed method.

Formulation of AMD control systems with fault signal

When several accelerometers fail to work, the system is considered to introduce a time-varying fault signal f and is assumed to follow the form described in ref. 26. The force equilibrium of the flexible buildings (n degrees of freedom) with an AMD system is

$$M\ddot{X}(t) + C\dot{X}(t) + KX(t) = B_w w(t) + B_s u(t) + B_e f(t), \quad (1)$$

where M, C and K are the mass matrix, damping matrix and stiffness matrix of the system respectively. u and w are the control force and strong wind respectively. B_s, B_w and B_e are the position matrices of control force, strong wind and fault signal respectively. $\ddot{X}(t)$, $\dot{X}(t)$ and $X(t)$ are the acceleration, velocity and displacement vector of the system respectively.

The degrees of freedom of the whole control system (a building and its AMD system) become (n + 1). The state vectors $Z = [X \quad \dot{X}]^T$ of the system include displacement and velocity. Therefore, its dimension is $2 \times (n + 1)$. Its derivative, which includes velocity and acceleration, is $\dot{Z} = [\dot{X} \quad \ddot{X}]^T$. Equation (1) can be expressed into the state equation as

$$\dot{Z}(t) = AZ(t) + B_1 w(t) + B_2 u(t) + Ef(t);$$

$$A = \begin{bmatrix} 0 & I \\ -M^{-1}K & -M^{-1}C \end{bmatrix}_{2(n+1)\times 2(n+1)},$$

$$B_1 = \begin{bmatrix} 0 \\ -M^{-1}B_w \end{bmatrix}_{2(n+1)\times(n+1)},$$

$$B_2 = \begin{bmatrix} 0 \\ -M^{-1}B_s \end{bmatrix}_{2(n+1)\times 1}, E = \begin{bmatrix} 0 \\ -M^{-1}B_e \end{bmatrix}_{2(n+1)\times(n+1)}, \quad (2)$$

where A, B_1 and B_2 are the state matrix, the excitation matrix and the control matrix respectively. E is the influence matrices of the fault signal on system state equation.

The observation equation can output displacement, velocity and acceleration of the system. The displacement and velocity are used to verify the control effectiveness, and the acceleration is used to observe the whole system state.

$$Y(t) = CZ(t) + D_1 w(t) + D_2 u(t) + Ff(t);$$

$$C = \begin{bmatrix} I & 0 \\ 0 & I \\ -M^{-1}K & -M^{-1}C \end{bmatrix}_{3(n+1)\times 2(n+1)}$$

$$D_1 = \begin{bmatrix} 0 \\ 0 \\ -M^{-1}B_w \end{bmatrix}_{3(n+1)\times(n+1)},$$

$$D_2 = \begin{bmatrix} 0 \\ 0 \\ -M^{-1}B_s \end{bmatrix}_{3(n+1)\times 1}, \quad F = \begin{bmatrix} 0 \\ 0 \\ -M^{-1}B_e \end{bmatrix}_{3(n+1)\times(n+1)}, \quad (3)$$

where Y is the output vector, and C, D_1 and D_2 are the state output matrix, the direct transmission matrices of control force and external excitation respectively. F is the influence matrix of the fault signal on system observation equation.

The system shown as eq. (3) can be illustrated by Figure 1 *a*. P is the mathematical model of eq. (3), and C_o is the controller. When the fault signal exists in certain sensors, an input signal f is added into the system and negatively impacts the performance of the control system.

Dynamic FTC controller design

Dynamic FDI filter

In order to guarantee the performance of the control system under the influence of the fault signal, the dynamic FDI filter C_D is required to detect and isolate the fault signal in time. The output information of the system is used as the input of C_D. Since the external excitation input W and the fault signal f are unknown, the output measurement Y and the detected fault signal r are regarded as the input and output of C_D respectively. The error signal $e = r - f$ is introduced to evaluate the

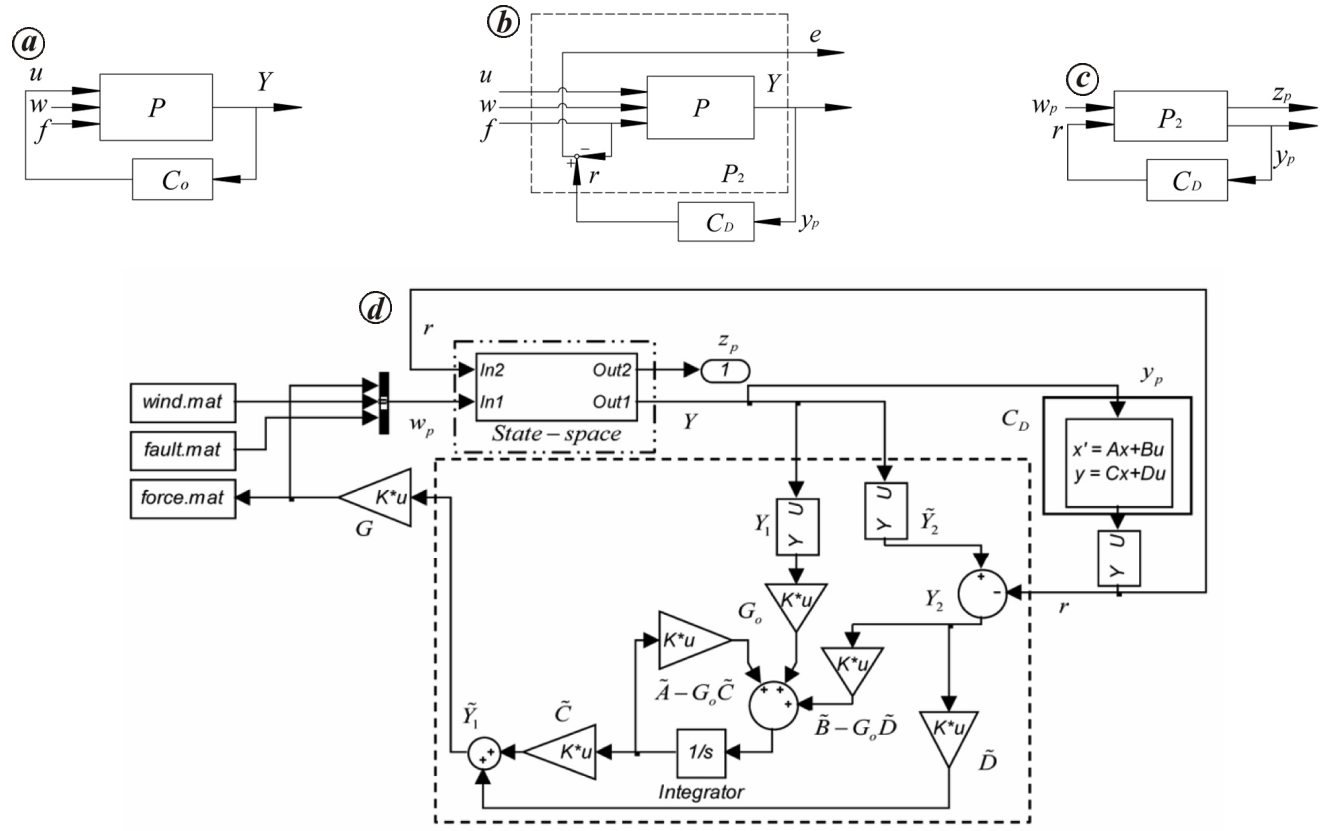

Figure 1. Block diagram of different systems: ***a***, The system with fault signal; ***b***, The dynamic FDI system I; ***c***, The dynamic FDI system II; ***d***, The dynamic FTC system.

performance of C_D. If the error signal is close to zero, it means the output of C_D is close to the actual fault signal. The design block diagram of C_D is shown in Figure 1 *b*, and P_2 inside the dashed box in Figure 1 *b* represents the space-state model for designing the dynamic FDI system.

Supposing $w_p = [u \quad w \quad f]^T$, $y_p = Y$ and $z_p = e$, then the state-space equation of the system is shown in Figure 1 *c* and is described as

$$\begin{cases} \dot{Z}(t) = AZ(t) + B_{1p}w_p(t) + B_{2p}r(t) \\ z_p(t) = C_{1p}Z(t) + D_{11p}w_p(t) + D_{12p}r(t) \\ y_p(t) = C_{2p}Z(t) + D_{21p}w_p(t) + D_{22p}r(t) \end{cases}, \tag{4}$$

where $B_{1p} = [B_2 \quad B_1 \quad E]$, $B_{2p} = 0$, $C_{1p} = 0$, $C_{2p} = C$, $D_{11p} = [0 \quad 0 \quad -I]$, $D_{12p} = I$, $D_{21p} = [D_2 \quad D_1 \quad F]$ and $D_{22p} = 0$ respectively.

Equation (4) is represented by the block diagram shown in Figure 1 *c*. The design of the FDI filter is transformed into the design problem of a controller. Specifically, the controller C_D is designed to guarantee that the response of the augmented system P_2 under the effect of disturbance w_p is minimum. The aim is to use H_2/H_∞ control theory to design the dynamic FDI filter. Specifically, the difference z_p between the estimated and actual fault signals is regarded as the target output, and the designers should guarantee that H_2 norms of the transfer function between the interference input w_p and the target output z_p is minimum.

The input of C_D is $y_p = Y$, the output is the detected fault signal r, and the state-space equation of C_D is

$$\begin{cases} \dot{Z}_f = A_f Z_f + B_f y_p \\ r = C_f Z_f + D_f y_p \end{cases}, \tag{5}$$

where Z_f is the state vectors of C_D.

To eliminate r and y_p in eq. (5), supposing $Z_{CL} = [Z \quad Z_f]^T$, then eqs (4) and (5) are combined into a new closed-loop system as

$$\begin{cases} \dot{Z}_{CL} = A_{CL}Z_{CL} + B_{CL}w_p \\ z_p = C_{CL}Z_{CL} + D_{CL}w_p \end{cases}, \tag{6}$$

where

$$A_{CL} = \begin{bmatrix} A & 0 \\ B_f C_{2p} & A_f \end{bmatrix}, \quad B_{CL} = \begin{bmatrix} B_{1p} \\ B_f D_{21p} \end{bmatrix},$$

$$C_{CL} = [D_f C_{2p} \quad C_f], \quad D_{CL} = D_{11p} + D_f D_{21p}. \tag{7}$$

The control system shown as eq. (4) has a H_∞ FDI filter[27], if and only if there exists a symmetric positive-definite matrix P such that the following inequality holds

$$\begin{bmatrix} A_{CL}^T P + PA_{CL} & PB_{CL} & C_{CL}^T \\ B_{CL}^T P & -I & D_{CL}^T \\ C_{CL} & D_{CL} & -\gamma^2 I \end{bmatrix} < 0. \tag{8}$$

where A_{CL}, B_{CL}, C_{CL} and D_{CL} are determined by eq. (7) and γ is a given positive constant. However, because inequality (8) is a nonlinear matrix inequality of the variables P, A_f, B_f, C_f and D_f, it is difficult to obtain the feasible matrix variables from the inequality directly. Therefore, the variable substitution method[24] needs to be used to transform the nonlinear matrix inequality (8) into a linear matrix inequality, and then the LMI toolbox can be used to solve the problem.

P and its inverse matrix P^{-1} are written as the block matrices

$$P = \begin{bmatrix} P_{11} & P_{12} \\ P_{12}^T & P_{22} \end{bmatrix}, P^{-1} = \begin{bmatrix} S_{11} & S_{12} \\ S_{12}^T & S_{22} \end{bmatrix}, \tag{9}$$

where $P_{11} \in R^{n\times n}$ and $S_{11} \in R^{n\times n}$. Supposing $I = P \cdot P^{-1}$, then

$$I = P_{11}S_{11} + P_{12}S_{12}^T. \tag{10}$$

Supposing

$$J = \begin{bmatrix} S_{11} & I \\ S_{12}^T & 0 \end{bmatrix}, \ \bar{J} = \begin{bmatrix} I & P_{11} \\ 0 & P_{12}^T \end{bmatrix}. \tag{11}$$

Supposing $PJ = \bar{J}$. Then

$$J^T PA_{CL}J = \begin{bmatrix} AS_{11} & A \\ P_{11}AS_{11} + P_{12}B_f C_{2p}S_{11} + P_{12}A_f S_{12}^T & P_{11}A + P_{12}B_f C_{2p} \end{bmatrix},$$

$$J^T PB_{CL} = \begin{bmatrix} B_{1p} \\ P_{11}B_{1p} + P_{12}B_f D_{21p} \end{bmatrix},$$

$$J^T C_{CL}^T = \begin{bmatrix} S_{11}C_{2p}^T D_f^T + S_{12}C_f^T \\ C_{2p}^T D_f^T \end{bmatrix}. \tag{12}$$

Supposing

$$L = P_{12}B_f, \tilde{L} = C_f S_{12}^T, \hat{L} = P_{12}A_f S_{12}^T. \tag{13}$$

Both sides of the matrix inequality (8) are pre- and post-multiplying $\mathrm{diag}\{J^T, I, I\}$ and $\mathrm{diag}\{J, I, I\}$ respectively. Then the matrix inequality (8) is

$$\begin{bmatrix} \begin{pmatrix} AS_{11} + \\ S_{11}A^T \end{pmatrix} & \begin{pmatrix} A + S_{11}A^T P_{11} + \\ S_{11}C_{2p}^T L^T + \hat{L}^T \end{pmatrix} & B_{1p} & \begin{pmatrix} (S_{11}C_{2p}^T D_f^T \\ + \tilde{L}^T) \end{pmatrix} \\ * & \begin{pmatrix} A^T P_{11} + P_{11}A + \\ C_{2p}^T L^T + LC_{2p} \end{pmatrix} & \begin{pmatrix} (P_{11}B_{1p} + \\ LD_{21p}) \end{pmatrix} & C_{2p}^T D_f^T \\ * & * & -I & \begin{pmatrix} (D_{11p}^T \\ + D_{21p}^T D_f^T) \end{pmatrix} \\ * & * & * & -\gamma^2 I \end{bmatrix} < 0. \tag{14}$$

The sub elements '*' of the upper matrix inequality can be obtained according to the symmetry of the matrix. The matrix inequality (14) is pre- and post-multiplying $\mathrm{diag}\{S_{11}^{-1}, I, I, I\}$, then

$$\begin{bmatrix} \begin{pmatrix} (S_{11}^{-1}A \\ + A^T S_{11}^{-1}) \end{pmatrix} & \begin{pmatrix} S_{11}^{-1}A + A^T P_{11} \\ + C_{2p}^T L^T + S_{11}^{-1}\hat{L}^T \end{pmatrix} & S_{11}^{-1}B_{1p} & \begin{pmatrix} (C_{2p}^T D_f^T \\ + S_{11}^{-1}\tilde{L}^T) \end{pmatrix} \\ * & \begin{pmatrix} A^T P_{11} + P_{11}A \\ + C_{2p}^T L^T + LC_{2p} \end{pmatrix} & \begin{pmatrix} (P_{11}B_{1p} \\ + LD_{21p}) \end{pmatrix} & C_{2p}^T D_f^T \\ * & * & -I & \begin{pmatrix} (D_{11p}^T + \\ D_{21p}^T D_f^T) \end{pmatrix} \\ * & * & * & -\gamma^2 I \end{bmatrix} < 0. \tag{15}$$

Supposing

$$R = S_{11}^{-1}, X = P_{11}, M = \hat{L}R, N = \tilde{L}R. \tag{16}$$

Then, the inequality (15) is

$$\begin{bmatrix} RA + A^T R & \begin{pmatrix} RA + A^T X + \\ C_{2p}^T L^T + M^T \end{pmatrix} & RB_{1p} & \begin{pmatrix} (C_{2p}^T D_f^T \\ + N^T) \end{pmatrix} \\ * & \begin{pmatrix} A^T X + XA + \\ C_{2p}^T L^T + LC_{2p} \end{pmatrix} & \begin{pmatrix} (XB_{1p} + \\ LD_{21p}) \end{pmatrix} & C_{2p}^T D_f^T \\ * & * & -I & \begin{pmatrix} (D_{11p}^T + \\ D_{21p}^T D_f^T) \end{pmatrix} \\ * & * & * & -\gamma^2 I \end{bmatrix} < 0. \tag{17}$$

The matrix P is a positive-definite matrix, if and only if the following inequality is established.

$$J^T PJ = \begin{bmatrix} S_{11} & I \\ I & P_{11} \end{bmatrix} > 0. \tag{18}$$

Then

$$P_{11} - S_{11}^{-1} = X - R > 0, \tag{19}$$

where R, X, M, N, L and D_f are the feasible solutions of the matrix inequalities (17) and (19).

Similarly, η is a given positive constant, if and only if there exists symmetric positive-definite matrices P and Q such that the following inequalities hold.

$$A_{CL}P^{-1} + P^{-1}A_{CL}^T + B_{CL}B_{CL}^T < 0, \tag{20}$$

$$\begin{bmatrix} -Q & C_{CL}P^{-1} \\ P^{-1}C_{CL}^T & -P^{-1} \end{bmatrix} < 0, \tag{21}$$

$$\text{trace}(Q) < \eta^2. \tag{22}$$

The control system shown as eq. (4) has a H_2 FDI filter[24]. The inequality (20) is satisfied by the inequality (8). The matrix inequality (21) is pre- and post-multiplying $\text{diag}\{I, P\}$, then

$$\begin{bmatrix} -Q & C_{CL} \\ C_{CL}^T & -P \end{bmatrix} < 0. \tag{23}$$

The matrix inequality (23) is pre- and post-multiplying $\text{diag}\{I, J^T\}$ and $\text{diag}\{I, J\}$ respectively. According to eq. (12), the matrix inequality (23) is equivalent to

$$\begin{bmatrix} -Q & D_f C_{2p} S_{11} + C_f S_{12}^T & D_f C_{2p} \\ * & -S_{11} & -I \\ * & * & -P_{11} \end{bmatrix} < 0. \tag{24}$$

The matrix inequality (24) is pre- and post-multiplying $\text{diag}\{I, S_{11}^{-1}, I\}$, then

$$\begin{bmatrix} -Q & D_f C_{2p} + C_f S_{12}^T S_{11}^{-1} & D_f C_{2p} \\ * & -S_{11}^{-1} & -S_{11}^{-1} \\ * & * & -P_{11} \end{bmatrix} < 0. \tag{25}$$

Using the variable substitution method[24], variables are defined as eqs (13) and (16); then the matrix inequality (25) is equivalent to

$$\begin{bmatrix} -Q & D_f C_{2p} + N & D_f C_{2p} \\ * & -R & -R \\ * & * & -X \end{bmatrix} < 0, \tag{26}$$

where R, X, H, N and D_f are the feasible solutions of the matrix inequalities (26) and (22).

Therefore, γ and η are given positive constants for the control system shown as eq. (6) that has a dynamic FDI filter, if and only if the optimization problem is established.

$$\min_{R,X,M,Z,N,Q} \eta, \tag{27}$$

s.t. (1) Inequality (17); (2) Inequality (19); (3) Inequality(26); (4) Inequality(22); where R, X, M, Q, N, L and D_f are the feasible solutions of the matrix inequalities (27). According to eqs (13) and (16), we get

$$A_f = P_{12}^{-1}\hat{L}(S_{12}^T)^{-1}, B_f = P_{12}^{-1}L, C_f = \tilde{L}(S_{12}^T)^{-1}. \tag{28}$$

The transfer function of the dynamic FDI filter is

$$\begin{aligned} H(s) &= C_f(sI - A_f)^{-1}B_f + D_f \\ &= \tilde{L}(S_{12}^T)^{-1}[sI - P_{12}^{-1}\hat{L}(S_{12}^T)^{-1}]P_{12}^{-1}L + D_f. \end{aligned} \tag{29}$$

According to eq. (10), eq. (29) is equivalent to

$$\begin{aligned} H(s) &= \tilde{L}[s(P_{12}S_{12}^T) - \hat{L}]^{-1}L + D_f \\ &= \tilde{L}[s(I - P_{11}S_{11}) - \hat{L}]^{-1}L + D_f \\ &= N[s(R - X) - M]^{-1}L + D_f \\ &= N[sI - (R - X)^{-1}M]^{-1}[(R - X)^{-1}L] + D_f. \end{aligned} \tag{30}$$

Then

$$A_f = (R - X)^{-1}M, B_f = (R - X)^{-1}L, C_f = N, \tag{31}$$

and D_f are the coefficient matrices of the dynamic FDI filter C_D shown as eq. (5) for the control system shown as eq. (4).

Dynamic FTC controller with a state observer and a FDI filter

The nonlinear matrix inequalities are transformed into the form of LMI based on the variable substitution method,

and the solver 'feasp' of LMI toolbox in MATLAB is used for solving the sub-optimal problem. The variables replaced by the method are restored, and then four coefficient matrices (A_f, B_f, C_f and D_f) of the dynamic FDI filter C_D are solved. The fault signal in sensors from measuring signal Y is detected and isolated by the FDI filter C_D. Based on these, a dynamic FTC controller can be built to control the structural responses. The control forces of the state feedback control system after fault isolation is calculated by region pole-assignment algorithm.

The control forces of the FTC controller are described as

$$u(t) = -G \cdot Z, \tag{32}$$

where G is a closed-loop feedback gain matrix based on regional pole-assignment algorithm[25].

By substituting eq. (32) into eq. (2), we get

$$\begin{cases} \dot{Z} = (A - B_2 G)Z + B_1 w(t) \\ Y = (C - D_2 G)Z + D_1 w(t) \end{cases}. \tag{33}$$

The state vector of each floor is estimated effectively by using the state observer. Supposing $\bar{A} = A - B_2 G$, $\bar{B} = B_1$, $\bar{C} = C - D_2 G$ and $\bar{D} = D_1$, and a brief form of eq. (33) is

$$\begin{cases} \dot{Z} = \bar{A}Z + \bar{B}w \\ Y = \bar{C}Z + \bar{D}w \end{cases}. \tag{34}$$

The second equation of eq. (34) is written in the form of a partitioned matrix.

$$\begin{Bmatrix} Y_1 \\ Y_2 \end{Bmatrix} = \begin{bmatrix} \bar{C}_1 \\ \bar{C}_2 \end{bmatrix} \cdot Z + \begin{bmatrix} \bar{D}_1 \\ \bar{D}_2 \end{bmatrix} \cdot w, \tag{35}$$

where Y_1 is a vector of displacement and velocity of the structure and its AMD. Y_2 is a vector of acceleration, which is processed by the FDI filter, and $Y_2 = \tilde{Y}_2 - r$, $\tilde{Y}_2$ is the acceleration response with fault signal.

According to eq. (35), the external excitation vector can be written as

$$w = \bar{D}_2^{-1} \cdot (Y_2 - \bar{C}_2 Z). \tag{36}$$

By substituting eq. (36) into eqs (34) and (35), we get

$$\begin{cases} \dot{Z} = (\bar{A} - \bar{B}\bar{D}_2^{-1}\bar{C}_2)Z + \bar{B}\bar{D}_2^{-1}Y_2 \\ Y_1 = (\bar{C}_1 - \bar{D}_1\bar{D}_2^{-1}\bar{C}_2)Z + \bar{D}_1\bar{D}_2^{-1}Y_2 \end{cases}. \tag{37}$$

Supposing $\tilde{A} = \bar{A} - \bar{B}\bar{D}_2^{-1}\bar{C}_2$, $\tilde{B} = \bar{B}\bar{D}_2^{-1}$, $\tilde{C} = \bar{C}_1 - \bar{D}_1\bar{D}_2^{-1}\bar{C}_2$ and $\tilde{D} = \bar{D}_1\bar{D}_2^{-1}$, eq. (37) can be written as

$$\begin{cases} \dot{Z} = \tilde{A}Z + \tilde{B}Y_2 \\ Y_1 = \tilde{C}Z + \tilde{D}Y_2 \end{cases}. \tag{38}$$

The state observer is described as

$$\begin{cases} \dot{Z} = \tilde{A}Z + \tilde{B}Y_2 + G_o(Y_1 - \tilde{Y}_1) \\ \tilde{Y}_1 = \tilde{C}Z + \tilde{D}Y_2 \end{cases}. \tag{39}$$

By substituting the second equation of eq. (39) into the first equation, Y_2 and Z can be used to estimate the system state vectors $\tilde{Y}_1$.

$$\begin{cases} \dot{Z} = (\tilde{A} - G_o\tilde{C})Z + (\tilde{B} - G_o\tilde{D})Y_2 + G_o Y_1 \\ \tilde{Y}_1 = \tilde{C}Z + \tilde{D}Y_2 \end{cases}, \tag{40}$$

where G_o is the feedback gain of the observer. $\tilde{Y}_1$, which is an estimated vector of the system state of the structure and its AMD, is used to calculate the control force.

Based on the derivation above, the process of the FTC control system is illustrated in Figure 1 *d*. The state-space eq. (4) is shown by the point-line box, the state observer based on acceleration responses is depicted by the dashed box, and the symbol inside the black solid box represents the dynamic FDI filter C_D.

Numerical verification

In this paper, a ten-storey frame is constructed for numerical analysis. The height and total mass of this structure are 33 m and 892.9 tonnes respectively. The lumped mass method is used to build the mass matrix for the structure. A unit force is applied to each particle floor of the structure, and the displacement at each floor is then obtained and combined into the flexibility matrix. The stiffness matrix can be easily obtained, as the inverse of the flexibility matrix. The AMD control device is assumed to be installed on the eighth floor and is only used to control the horizontal vibration along the minor axis. Key parameters of AMD are listed in Table 1. Structural frequencies and modal mass participating ratios[28] of the ten-storey frame, which are calculated using the model constructed in Matlab, are listed in Table 2.

Based on Davenport spectrum, a ten-year return period fluctuating wind speed is generated for numerical analysis. Mixed autoregressive-moving average (MARMA) model[29] is proposed to simulate the stochastic process. The fluctuating wind load on each floor is calculated by eq. (41).

$$P_i = \rho \bar{V}(z) u_i(z,t) \mu_s S, \tag{41}$$

where P_i is the fluctuating wind load at ith floor, ρ the air density, $\bar{V}(z)$ the average wind speed at ith floor, u_i the

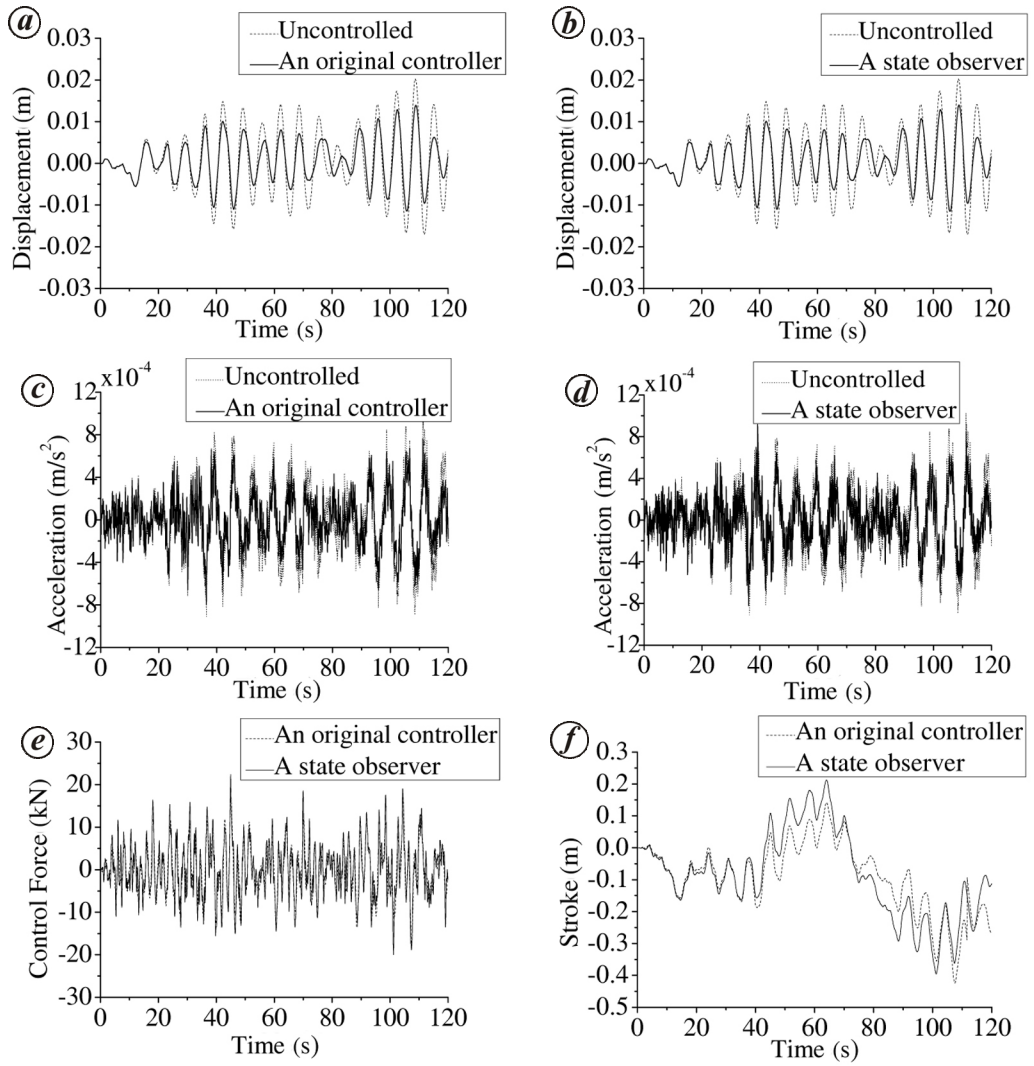

Figure 2. Comparison of the structural responses to 8th floor and the AMD parameters, controlled by an original controller (***a***) displacements and (***c***) accelerations, controlled by a state observer (***b***) displacements and (***d***) accelerations. ***e***, AMD control forces; ***f***, AMD strokes.

Table 1. Key parameters of AMD

Index	AMD
Auxiliary mass (kg)	4000
Effective stroke (m)	±1.1
Maximum driving force (kN)	27.5

Table 2. Modal mass participating ratios and natural frequencies of the frame

Order	Modal mass participation ratio	Frequency (Hz)
1	0.7940	0.1435
2	0.0985	0.4577
3	0.0410	0.8479
4	0.0237	1.3404
5	0.0156	1.9514

fluctuating wind speed that is associated with height and time. μ_s and S are the shape factor of a building and the area of windward side respectively.

Under the above ten-year return period wind load, an original controller and a state observer, both based on regional pole-assignment algorithm are designed for the ten-storey frame. The structural responses of the eighth floor, and AMD parameters of different systems are shown in Figure 2. Table 3 presents the maximum responses, control effects and values of AMD parameters. In this paper, the control effect is quantified as the ratio between dynamic responses of the structure with and without control, and AMD parameters include control force and stroke.

Figure 2 and Table 3 show that the original controller and the state observer, both based on pole-assignment algorithm, obviously reduce the wind vibration response.

Table 3. Comparison of control effects

Index		An original controller			A state observer		
		Displacement	Velocity	Acceleration	Displacement	Velocity	Acceleration
Control effect (%)	8th floor	34.4676	34.8078	30.4391	34.3121	34.7876	29.6056
	9th floor	34.4944	34.9371	30.0382	34.2934	34.7240	28.2551
	10th floor	34.5024	34.8192	27.5249	34.2621	34.6135	24.8263
AMD control forces (kN)			6.1413			6.3121	
AMD strokes (m)			0.1333			0.1324	

Specifically, the maximum variations of the displacement, velocity and acceleration control effects between two different systems are only 0.24%, 0.21% and 2.70%, and the AMD parameters of the state observer increase by 0.1708 N and –0.0009 m. Therefore, the acceleration response obtained from the optimal placement scheme of sensors is rationally used as a feedback signal for the state observer that also can guarantee that the system has the same superior control effect and stable AMD parameters as the original controller.

A dynamic FTC controller with a state observer and a FDI filter is then designed for the ten-storey frame. The accelerometer in the seventh floor is assumed to fail to work, and three forms of artificially added fault signals are assumed, i.e. square wave (the amplitude of 1 m/s^2, the period of 2 s and the width of 1 s), sine wave (the amplitude of 1 m/s^2, the period of 2 s) and white Gaussian noise (the power is 0.1 dBW, the load impedance is 0.1 Ω), as shown in Figure 3 *a–c*. The dimension of the fault signal $f(t)$ of the ten-storey frame is 11×1. The signals shown in Figure 3 *a–c* are added in the seventh floor's accelerometer. Time history analysis is achieved by simulink toolbox in Matlab, and the duration of the whole process is 600 s.

Under these scenarios, the effectiveness of the dynamic FDI filter is verified by comparing the detected fault signal with the artificially added one. The detected fault signals in seventh floor's accelerometer are shown in Figure 3 *d–f*, and the errors of added and detected fault signals in seventh floor's accelerometer are shown in Figure 3 *g–i*. Based on the results, under both conditions, the detected trend and amplitude of signals from the fault accelerometer are equal to the assumption. Moreover, Figure 3 *g–i* shows that the amplitudes of the errors are almost zero. Therefore, the FDI filter C_D designed in this paper is used to detect the location and the amplitude of the fault signal correctly.

The performance of the designed FTC controller is then verified by comparing with the system without fault signal (No fault signal). Under a ten-year return period wind load, the structural responses and the AMD parameters of different control systems with and without fault signal are shown in Figure 4. Fault signals with dynamic FTC stand for control systems with different time-varying fault signals (square wave, white Gaussian noise) and a dynamic FTC controller. In the figures, dashed lines represent the response of the structure without control under the wind load, and the solid lines show the response of the structure with control. The corresponding control effects (defined as the ratio between controlled and uncontrolled responses) and AMD parameters are listed in Table 4.

It can be seen that from Figure 4 and Table 4; (i) When the sensor has no fault signal, the controller based on regional pole-assignment algorithm effectively reduces the structural response. When the sensor fails, the control system that does not take the isolation measure is to diverge. Therefore, the fault signal in sensor cannot be ignored. The design of the dynamic FDI filter can isolate the fault signal, which is very important for the control system. (ii) When the sensor has a sine wave fault signal, the dynamic FTC controller effectively restrains the structural response, and its control effects are nearly equivalent to the system without a fault signal. Specifically, the maximum variations of the displacement, velocity and acceleration control effects between two different systems are only 0.06%, 0.05% and 0.17%. Therefore, the developed dynamic FTC controller effectively detects and isolates the fault signal. Also, the dynamic FTC controller maintains the stability of AMD parameters, which are consistent with the system without fault signal. Specifically, AMD parameters of the FTC controller increase only by 0.0046 N and 0.0086 m. The same result is obtained when the fault signal is white Gaussian noise.

Experimental verification

An experimental system of a four-storey steel frame with an AMD control device installed on the fourth floor is given in ref. 16. The acceleration signals of the second and fourth floors were used as the feedback signal for a controller to calculate the real-time control forces. A servo motor acquired the forces from an EtherCAT bus system and was used to add these forces to control the structure. The structural response signals of the second, third and fourth floors were used to verify the control effectiveness.

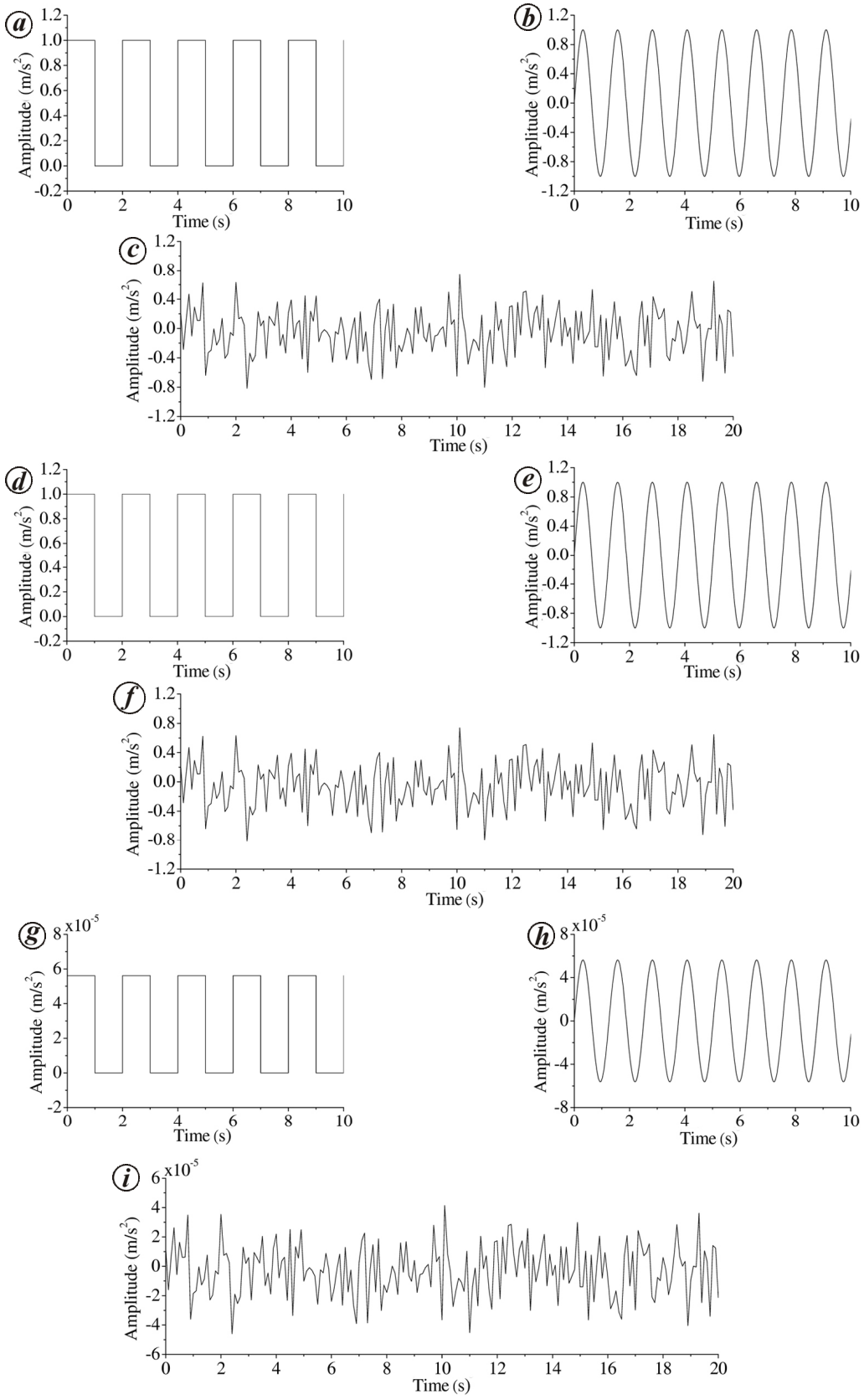

Figure 3. The artificially added fault signals in 7th floor's accelerometer: ***a***, Square wave; ***b***, Sine wave; ***c***, White Gaussian noise. The detected fault signals in 7th floor's accelerometer: ***d***, Square wave; ***e***, Sine wave; ***f***, White Gaussian noise. The errors z_p between two types of fault signals in 7th floor's accelerometer: ***g***, Square wave; ***h***, Sine wave; ***i***, White Gaussian noise.

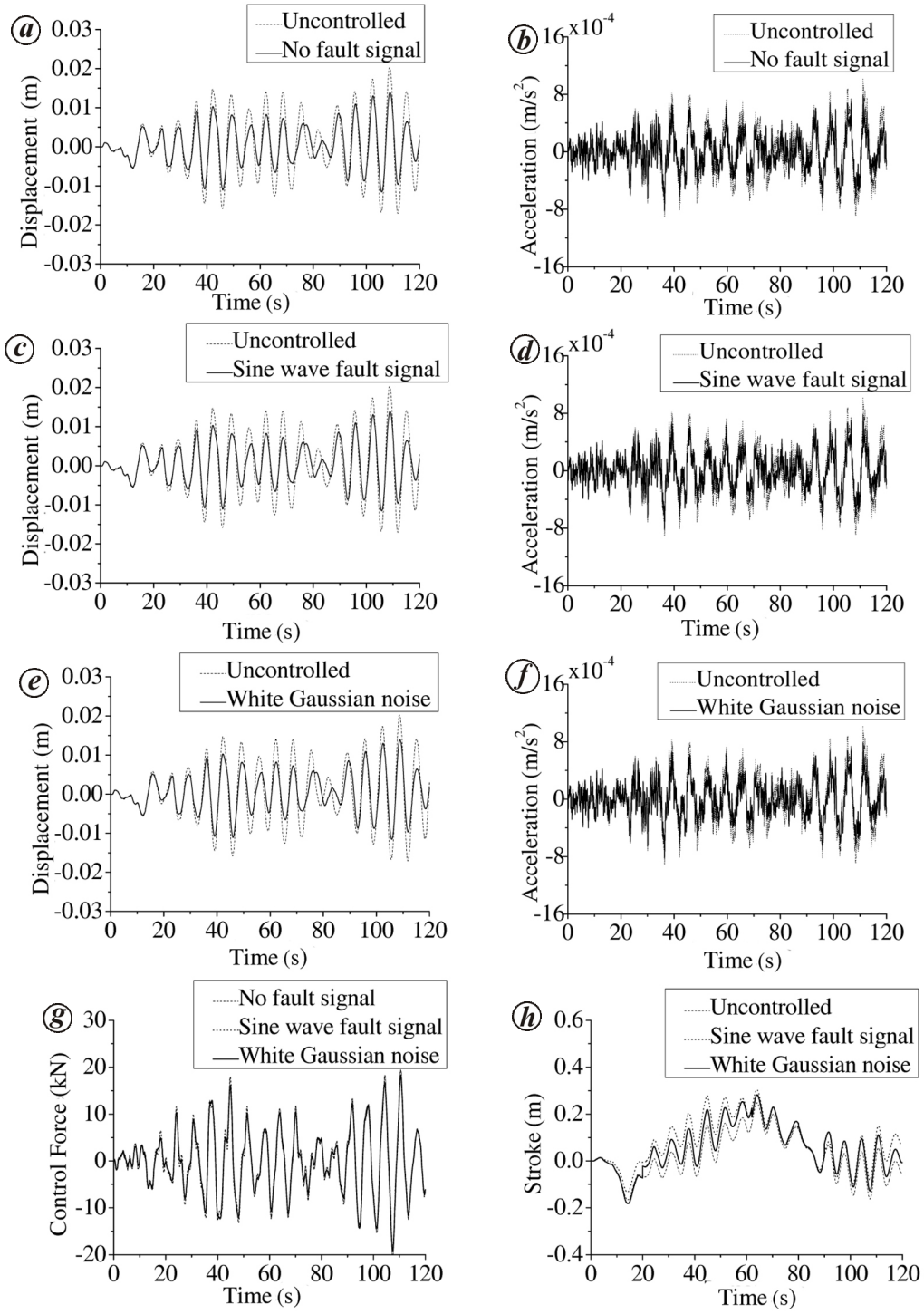

Figure 4. Comparison of the structural responses to 8th floor and the AMD parameters: ***a***, ***b***, Under uncontrolled and controlled without fault signal; ***c***, ***d***, Considering sine wave fault signal and controlled with dynamic FTC; ***e***, ***f***, Considering white Gaussian noise and controlled with dynamic FTC; ***g***, AMD control forces; ***h***, AMD strokes.

To verify the efficiency of the developed method, the FTC controller is applied to the experimental system. The original signal is monitored by the second, fourth floor acceleration response of the controlled structure. Then the observer is used to get estimated states to calculate the control forces. The loading frequency of the system is 1 Hz, that is, the peak value of the corresponding excitation force is 45.89 N, and the wave form of this force is sinusoidal. Under the above excitation load, the estimated and measured values of the structural responses are

Table 4. Comparison of control effects of the system with dynamic FTC (%)

Floor	Index	Without fault signal	With fault signal	With dynamic FTC	
				Sine wave	White Gaussian noise
8th	Displacement	33.6256	Divergent	33.5638	33.6434
	Velocity	33.8730	Divergent	33.8273	33.8723
	Acceleration	25.9426	Divergent	25.7753	25.7912
9th	Displacement	33.6092	Divergent	33.5480	33.6184
	Velocity	33.5387	Divergent	33.4949	33.4524
	Acceleration	25.4334	Divergent	25.5477	24.7110
10th	Displacement	33.5755	Divergent	33.5151	33.5761
	Velocity	32.9823	Divergent	32.9408	32.8127
	Acceleration	21.2427	Divergent	21.3326	20.2103
Control force (kN)		6.8985	Divergent	6.9031	6.7337
Stroke (m)		0.0925	Divergent	0.1011	0.1024

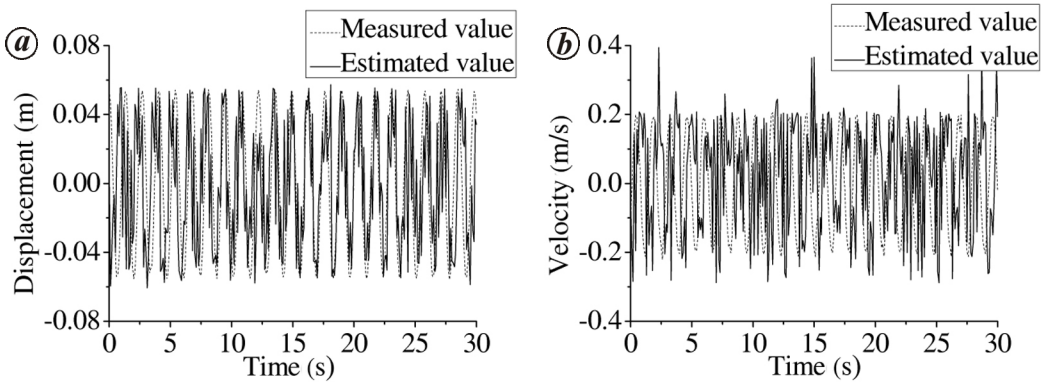

Figure 5. Comparison between measured and estimated system state in 4th floor: ***a***, Displacements; ***b***, Velocities.

showed in Figure 5. The duration of each scenario is 300 sec, and Figure 5 only gives data in 30 sec.

From Figure 5, it is seen that (i) The design method of the state observer based on the accelerations of partial floors is proposed in this paper, which estimates the whole state vectors of the system accurately. (ii) In the estimation results, the estimated displacement of the fourth floor is 0.0385 m, and in the actual results, the measured displacement is 0.0385 m, the displacement observation error is 0.4×10^{-3} m. The estimated velocity is 0.1479 m/s, the measured velocity is 0.1429 m/s, the velocity observation error is 0.5×10^{-2} m/s. Both the above two observation errors are really minor. (iii) There are two main reasons causing the observation errors of the displacement and velocity, (a) When the floor is moved to the place that has maximum horizontal displacement, the model has a slight and rapid vibration due to the coupling effect of vertical and horizontal sinusoidal loads. (b) There is a noise signal around the experimental system. It will affect if sensors can accurately measure the feedback signal or not.

When the accelerometer at the second floor fails to work, three forms of artificially added fault signals are assumed as shown in Figure 3 *a–c*. The detected fault accelerometer signal at second floor is shown in Figure 6. The detected fault accelerometer signals (square and sine wave) at the second floor changes with time, and the amplitudes (1.055989 m/s^2 and 1.055783 m/s^2) of the detected fault signals are close to the artificially added fault signal (1 m/s^2). For white Gaussian noise, the detected one is pretty close to the origin one. Therefore, the FDI filtered signed in this paper is used to detect the location and the amplitude of the fault signal correctly.

Choosing two types of fault signals (sine wave and white Gaussian noise) as an example, the structural responses of different control systems with and without FTC are shown in Figure 7, and the corresponding control effects and AMD parameters are listed in Table 5.

Based on the results, (1) AMD control system increases the structural response and plays a negative role when the sensor fails, if designers do not take any isolation measures. Specifically, the displacement and acceleration control effects of the system with fault signal are all negative numbers. Therefore, it is important to design a FTC controller with a state observer and a FDI filter to detect and isolate the fault signal. (2) For sine wave fault signal,

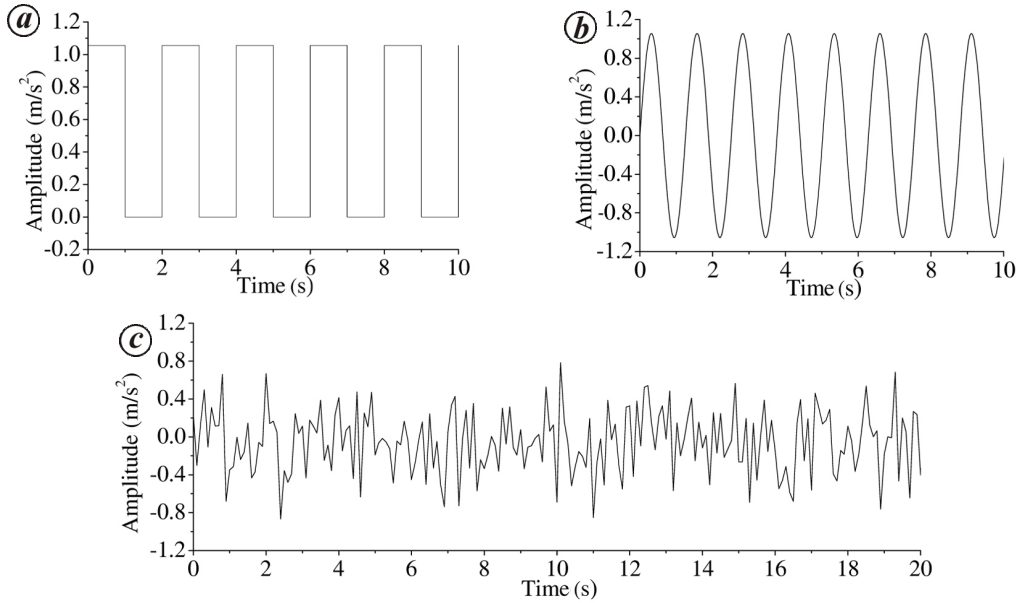

Figure 6. The detected fault signal in 2nd floor's accelerometer of the experimental system: ***a***, Square wave; ***b***, Sine wave; ***c***, White Gaussian noise.

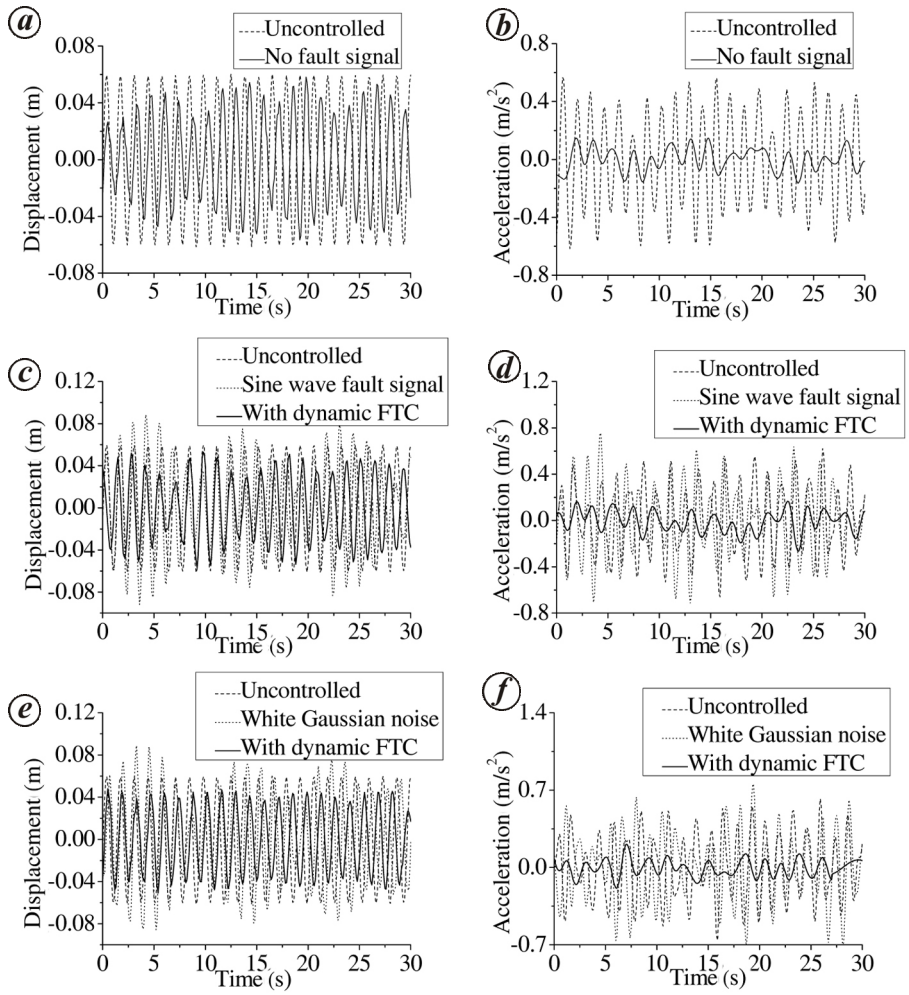

Figure 7. Comparison of the structural responses to 4th floor of the experimental system: ***a***, ***b***, Under uncontrolled and controlled without fault signal; ***c***, ***d***, Considering sine wave fault signal and controlled with dynamic FTC; ***e***, ***f***, Considering white Gaussian noise and controlled with dynamic FTC.

Table 5. Control effectiveness of structural responses (%)

Index		Without fault signal	With fault signal (Sine wave)		With fault signal (White Gaussian noise)	
			Without FTC	With FTC	Without FTC	With FTC
Displacement (m)	2nd floor	27.0551	–4.9037	24.1543	–11.1040	27.6251
	3rd floor	27.9837	–4.7445	24.7997	–10.6274	27.7734
	4th floor	28.1198	–4.7445	24.7997	–9.8088	29.5676
Acceleration(m/s^2)	2nd floor	76.4537	–10.1991	74.2183	–8.0170	72.9299
	3rd floor	40.7535	–7.5637	43.5798	–2.6597	47.3597
	4th floor	73.7438	–11.4507	70.2725	–7.4639	76.5141
Control forces (N)		32.2191	31.4122	34.8742	30.9310	29.0907
Strokes (m)		0.1692	0.1878	0.1484	0.1671	0.1429

control effects and AMD parameters of the FTC system are close to the system without fault signal. Specifically, the maximum variations of the displacement, velocity and acceleration control effects between two different systems are 3.32% and 3.47%, and the AMD parameters of the FTC controller increase by 2.66 N and –0.0208 m. For white Gaussian noise, the maximum variations of the different control effects between two different systems are 1.44% and 6.60%, and the AMD parameters decrease by 3.13 N and 0.0263 m. Therefore, the FTC controller detects and isolates the fault signal effectively, and also restrains the structural responses and maintains the AMD parameters in the appropriate range. (3) The structural response does not completely obey the sine law due to the interaction between the AMD system and the structure, and the coupling of the horizontal and the vertical structural vibrations. (4) AMD device is placed in the fourth floor of the structure. Further, the acceleration control needs high frequency control force that will mitigate the structural high-order modes. Therefore, the control effect of third floor, which has an opposite high-order phase with the fourth floor, is significantly less than the control effect of second and fourth floors.

Conclusions

In this paper, a state observer is designed for the considered problem, i.e. state vectors of the control system are difficult to directly measure. Moreover, the fault signal has a negative influence on the designed state observer. To address this issue, a dynamic FDI filter design method is presented to achieve the detection and isolation of the fault signal. Finally, a dynamic FTC controller design method that combines a state observer and a FDI filter is finished. A numerical example and an experiment are presented to verify the effectiveness of the proposed method. Based on the results, the following conclusions are drawn.

(1) A well-designed dynamic FDI filter is used to detect the location and the amplitude of the fault signal correctly.

(2) The state observer based on the accelerations of each floors, accurately observes the whole states of the system, and has superior control effect and stable AMD parameters.

(3) When the sensor fails to work, the system is regarded as introducing a new input signal that brings negative interference to the system. AMD control system without consideration of this issue increases the structural response when the fault signal in the sensor presents.

(4) The FTC controller is combined with a state observer and a dynamic FDI filter. It tolerates the fault signal in accelerometers, effectively controls the structural response and maintains the stability of AMD parameters. Its control effects and AMD parameters are close to the system without fault signal. Therefore, it enhances the robustness of the control system.

Even with fault signals, the control performances are still stable, as demonstrated by the above results. Therefore, the dynamic FTC controller described in the paper is regarded as robust control. The dynamic FDI filter designed in this paper is applied widely, but may have difficulties in achieving the process of fault-tolerance control in engineering practices through hardware devices. Thus, future efforts in this direction are focused on a static FDI filter shown as a gain matrix to achieve the conversion between the measuring output with fault signal and the real output.

1. Cao, H., Reinhorn, A. M. and Soong, T. T., Design of an active mass damper for a tall TV tower in Nanjing, China. *Eng. Struct.*, 1998, **20**, 134–143.
2. Yamamoto, M., Aizawa, S., Higashino, M. and Toyama, K., Practical applications of active mass dampers with hydraulic actuator. *Earthq. Eng. Struct. D*, 2001, **30**, 1697–1717.
3. Ricciardelli, F., Pizzimenti, A. D. and Mattei, M., Passive and active mass damper control of the response of tall buildings to wind gustiness. *Eng. Struct.*, 2003, **25**, 1199–1209.
4. Ikeda, Y., Sasaki, K., Sakamoto, M. and Kobori, T., Active mass driver system as the first application of active structural control. *Earthq. Eng. Struct. D*, 2001, **30**, 1575–1595.
5. Basu, B. *et al.*, A European association for the control of structures joint perspective. Recent studies in civil structural control across Europe. *Struct. Control Hlth.*, 2014, **21**, 1414–1436.

6. Chen, J. and Patton, R. J., *Robust Model-based Fault Diagnosis for Dynamics Systems*, Kluwer Academic Publishers, Boston, 1999.
7. Zhang, Y. M. and Jiang, J., Integrated active fault-tolerant control using IMM approach. *IEEE T Aero Elec. Syst.*, 2001, **37**, 1221–1235.
8. Polycarpou, M. M., Fault accommodation of a class of multivariable nonlinear dynamical systems. *IEEE Trans. Automat. Contr.*, 2001, **5**, 736–742.
9. Marx, B., Koenig, D. and Georges, D., Robust fault-tolerant control for descriptor systems. *IEEE Trans. Automat Contr.*, 2004, **49**, 1869–1875.
10. Mehra, R. K. and Peschon, J., Innovations approach to fault detection and diagnosis in dynamic systems. *Automatica*, 1971, **7**, 637.
11. Shao, S., Watson, A. J., Clare, J. C. and Wheeler, P. W., Robustness analysis and experimental validation of a fault detection and isolation method for the modular multilevel converter. *IEEE Trans. Power Electr.*, 2016, **31**, 3794–3805.
12. Rios, H., Davila, J., Fridman, L. and Edwards, C., Fault detection and isolation for nonlinear systems via high-order-sliding-mode multiple-observer. *Int. J. Robust Nonlin.*, 2015, **25**, 2871–2893.
13. Smarsly, K. and Law, K. H., Decentralized fault detection and isolation in wireless structural health monitoring systems using analytical redundancy. *Adv. Eng. Softw.*, 2014, **73**, 1–10.
14. Zhang, Z. and Jaimoukha, I. M., On-line fault detection and isolation for linear discrete-time uncertain systems. *Automatica*, 2014, **50**, 513–518.
15. Teng, J., Xing, H. B., Xiao, Y. Q., Liu, C. Y., Li, H. and Ou, J. P., Design and implementation of AMD system for response control in tall buildings. *Smart Struct. Syst.*, 2014, **13**, 235–255.
16. Teng, J., Xing, H. B., Lu, W., Li, Z. H. and Chen, C. J., Influence analysis of time delay to active mass damper control system using pole assignment method. *Mech. Syst. Signal Process.*, 2016, **80**, 99–116.
17. Jeon, S. and Tomizuka, M., Benefits of acceleration measurement in velocity estimation and motion control. *Control Eng. Pract.*, 2007, **15**, 325–332.
18. Song, G. B., Kelly, B., Agrawal, B. N., Lam, P. C. and Srivatsan, T. S., Application of shape memory alloy wire actuator for precision position control of a composite beam. *J. Mater. Eng. Perform*, 2000, **9**, 330–333.
19. Wang, Y., Time-delayed dynamic output feedback H_∞ controller design for civil structures: A decentralized approach through homotopic transformation. *Struct. Control Hlth.*, 2011, **18**, 121–139.
20. Caliskan, F. and Hajiyev, C., Aircraft sensor fault diagnosis based on Kalman filter innovation sequence. *Proceedings of the 37th IEEE Conference on Decision and Control (Cat. No.98CH36171)*, 1998, pp. 1313–1314.
21. Commault, C., Dion, J. M., Senante, O. and Motyeian, R., Observer-based fault detection and isolation for structured systems. *IEEE Trans. Automat. Contr.*, 2002, **47**, 2074–2079.
22. Saif, M. and Guan, Y. A new approach to robust fault-detection and identification. *IEEE Trans. Aerosp. Electron. Syst.*, 1993, **29**, 685–695.
23. Boyd, S., Ghaoui, L. E., Feron, E. and Balakrishnan, V., *Linear Matrix Inequalities in System and Control Theory*, Society for Industrial and Applied Mathematics, Philadelphia, Pennsylvania, 1994.
24. Yu, L., *Robust Control-Linear Matrix Inequalities Approach*, Tsinghua University Press, Beijing, 2002.
25. Haddad, W. M. and Bernstein, D. S., Controller-design with regional pole constraints. *IEEE Trans. Automat. Contr.*, 1992, **37**, 54–69.
26. Gao, Z. and Ding, S. X., State and disturbance estimator for time-delay systems with application to fault estimation and signal compensation. *IEEE Trans. Signal Process*, 2007, **55**, 5541–5551.
27. Gahinet, P. and Apkarian, P., A linear matrix inequality approach to h_∞ control. *Int. J. Robust Nonlin.*, 1994, **4**, 421–448.
28. Clough, R. W. and Penzien, J., *Dynamics of Structures*, US: McGraw-Hill Inc, 1975.
29. Hannan, E. J., The identification of vector mixed autoregressive-moving average system. *Biometrika*, 1969, **56**, 223–225.

ACKNOWLEDGEMENTS. The research described in this paper was financially supported by the Major International (Sino-US) Joint Research Project of the National Natural Science Foundation of China (Grant No. 51261120374), the National Natural Science Foundations of China (Grant No. 51378007 and 51538003), the Shenzhen Technology Innovation Programs (Grant No. JSGG20150330103937411 and JCYJ20150625142543473).

Received 9 October 2016; revised accepted 27 June 2017

doi: 10.18520/cs/v114/i02/341-354